*Int. J. Electrochem. Sci.*, 13 **(2018)** 11663 – 11674, doi: 10.20964/2018.12.12

**International Journal of ELECTROCHEMICAL SCIENCE**
www.electrochemsci.org

# Reduced Graphene Oxide-Doped Poly(N-alkyl-3,4-dihydrothieno[3,4-*b*][1,4]oxazine) with High Sensitivity of Indole-3-Acetic Acid

*Kai Qu*[1,§], *Shouli Ming*[1,§], *Haiyan Jia*[1], *Bin Guo*[2], *Ximei Liu*[3], *Nannan Jian*[1], *Guifang Niu*[3], *Baoyang Lu*[3,*] *and Jingkun Xu*[1,4*]

[1] School of Chemistry & Chemical Engineering, Jiangxi Science & Technology Normal University, Nanchang 330013, China
[2] College of Science, Nanjing Forestry University, Nanjing 210037 Jiangsu, China
[3] School of Pharmacy, Jiangxi Science & Technology Normal University, Nanchang 330013, China
[4] School of Chemistry and Molecular Engineering, Qingdao University of Science and Technology, Qingdao 266042, Shandong, China
[*]E-mail: lby1258@163.com; xujingkun1971@yeah.net
[§] These authors contributed equally to this work.

*Received:* 11 August 2018 / *Accepted:* 6 September 2018 / *Published:* 5 November 2018

A highly sensitive electrochemical sensor for detecting indole-3-acetic acid (IAA) was constructed based on the composite of poly(N-methyl-3,4-dihydrothieno[3,4-b][1,4]oxazine) (PMDTO) and reduced graphene oxide (RGO) (PMDTO/RGO). The PMDTO/RGO modified electrode was prepared by electrochemical polymerization of MDTO followed by the electrochemical reduction GO in their homogeneous aqueous solution. SEM demonstrated that PMDTO was covered with plate-like graphene through the two-step electrodeposition. The RGO, featuring large surface area and excellent conductivity, could not only improve the conductivity of the sensor, but also load more PMDTO to amplify the signal. The fabricated electrochemical sensor showed a low detection limit of $3\times10^{-8}$ M and a wide linear range from 0.1 to 10 μM for the recognition of IAA.

**Keywords:** poly(N-methyl-3,4-dihydrothieno[3,4-*b*][1,4]oxazine), sensor, indole-3-acetic acid, graphene oxide

## 1. INTRODUCTION

Indole-3-acetic acid (IAA), as a kind of plant hormones, plays an important role in plant growth processes including cell division, environmental response, gene expression and tissue decay [1,2]. Up to now, many techniques, such as solid-phase micro-extraction, vapor-phase extraction and liquid-

phase extraction [3,4], have been applied to detect IAA. These techniques exhibit good selection or sensitivity to the determination of IAA. However, the techniques also show some disadvantages, such as time-consuming and complex instruments. Compared to above techniques, the electrochemical analytical method with the advantages of high sensitivity, low cost, good selectivity, convenient apparatus and simple operation has attracted great attention [5-8].

In the fabrication progress of the electrochemical sensor, the interface modification is a crucial step, which influences the performances of the fabricated sensors. Various electrode materials, such as, gold nanoparticles (AuNPs), conducting polymers, grapheme and carbon nanotubes, have been used to detect minute quantities of IAA [5-10]. Among them, conducting polymers, especially PEDOT and its derivatives, show great promise in the application of electrochemical sensors due to the ease of structure modification towards great environmental stability and excellent electrical conductivity [11-15]. Moreover, the introduction of specific groups can make PEDOT derivatives exhibit high sensitivity for the detection.

Poly(N-methyl-3,4-dihydrothieno[3,4-b][1,4]oxazine) (PMDTO), a nitrogen derivative of PEDOT discovered recently [16], displays favorable optoelectronic properties and excellent electrochemical stability even in the aqueous system (keep 86% after 2000 cycles) [17]. Moreover, PMDTO could be easily prepared in aqueous system at a very low potential (the onset oxidation potential: 0.19 V *vs.* Ag/AgCl) [18]. However, pure PMDTO possess small specific surface area, which may impact the detection property. To solve this problem, active materials like carbon-based nanomaterials can be introduced into PMDTO matrix. Graphene, a two-dimensional (2D) nanomaterial of $sp^2$-hybridized carbon, possesses high surface area, unique electronic properties, high chemical and thermal stability, which is quite suitable for compositing. Moreover, many polymers and graphene compounds have been used to fabricate the electrochemical sensors for detecting heavy metal ions, pharmaceutical formulation and glucose, displaying low detection limits and wide linear ranges [19-27].

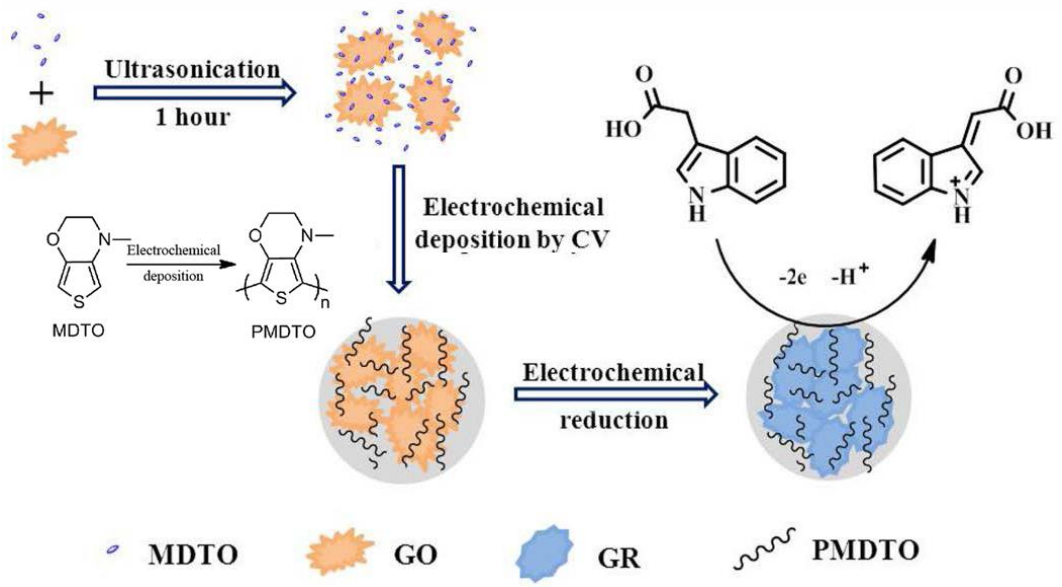


**Scheme 1.** The preparation process of PMDTO/RGO/GCE.

Herein, we composite poly(N-methyl-3,4-dihydrothieno[3,4-b][1,4]oxazine) (PMDTO) with reduced graphene oxide (RGO) through a two-step electrodeposition. Based on the composite PMDTO/RGO film, we construct a highly sensitive electrochemical sensor for detecting indole-3-acetic acid (IAA) (Scheme 1). In order to improve the selectivity, the as-prepared PMDTO/GO composite is reduced in 0.1 M $LiClO_4$ aqueous solution to shave a part of attaching functional groups. Additionally, the functions of GO and RGO are comparatively investigated by electrochemical impedance spectroscopy (EIS), scanning electron microscope (SEM) and cyclic voltammetry (CV). The fabricated sensor exhibits a wide linearity range (0.1~10 μM) and a low detection limit (0.03 μM), indicating potential usage of PMDTO in electrochemical sensors.

## 2. EXPERIMENTTAL

### *2.1 Chemicals*

Indole-3-acetic acid stock solution (10 mM) (IAA, Energy Chemical Co., Ltd) was prepared in ethanol. MDTO was synthesized via a one-step route based on previous reports [16-18]. Graphene oxide (GO, 99.8%; Nanjing XFNANO Materials Tech Co., Ltd.) was dispersed in DI water. The phosphate buffered solution (PBS) was prepared with disodium hydrogen phosphate dodecahydrate and sodium dihydrogen phosphate dihydrate (Sinopharm Chemical Reagent Co. Ltd.). Other reagents were all analytical grade and used without further purification.

### *2.2 Apparatuses*

Electrochemical experiments were studied at room temperature in a three-electrode system by a CHI660B electrochemical workstation (Shanghai Chenhua Co., Ltd., China). Glassy carbon electrode (GCE, Φ = 3 mm), Ag/AgCl electrode and platinum wire (Φ = 1 mm) were used as the working electrode, reference electrode and counter electrode, respectively. The structure characterization of PMDTO, PMDTO/GO and PMDTO/RGO was determined by Raman spectroscopy (Renishaw InVia-Reflex with a 633 nm laser). VEGA II-LSU scanning electron microscope (Tescan) was used to perform the SEM images. The pH of the solution was measured by a Delta 320 pH meter (Mettler-Toledo Instrument, Shanghai, China). The addition of sample was carried out by a micro-syringe (Shanghai Gaoge Industry & Trade Co. Ltd., China).

### *2.3 Preparation of PMDTO/RGO modified electrode*

GCE was polished with 0.05 μm alumina/water slurry on the chamois leather before the electrodeposition, then rinsed with distilled water and sonicated in distilled water and ethanol for 5 min, and finally dried in air. PMDTO/GO modified electrode (PMDTO/GO/GCE) was prepared in the homogeneous aqueous solution of MDTO (0.01 M) and GO (2.0 mg $mL^{-1}$) by cyclic voltammetry (CV), as shown in Fig. 1B. The PMDTO/RGO modified electrode (PMDTO/RGO/GCE) was

constructed by electrochemical reduction GO on PMDTO/GO/GCE by CV (-1.5 V~-0.2 V) in 0.1 mol $L^{-1}$ $LiClO_4$ aqueous solution.

### *2.4 Electrochemical performance*

The electron transfer number (n) in IAA oxidation process was determined by cyclic voltammograms (CVs) in 0.05 mM IAA and 0.1 M PBS (pH = 3.0) at different scan rates, and calculated using the Laviron's model [9], as the following equation:

$$E_{pa} = E^0 + \frac{RT}{\alpha nF}\ln\left(\frac{RTk_s}{\alpha nF}\right) + \frac{RT}{\alpha nF}\ln \nu$$

where $E_{pa}$ represents the anodic peak potential; $E^0$ represents the formal redox potential; □ represents the transfer coefficient, and its value is generally assumed to be 0.5 in a fully irreversible electrode process; $k_s$ represents the standard rate constant of the whole reaction; *v* represents the scan rate; *R* represents the gas constant; *T* is the absolute temperature; and *F* is the Faraday constant.

### *2.5 Determination of IAA*

Linear sweep voltammetry (LSV) was employed for quantitative assay of IAA under optimal conditions. The limitation of detection (LOD) [8] was defined as LOD = $3\sigma/S$, where $\sigma$ is the standard deviation of 20 parallel tests in 0.1 M PBS, and *S* is the slope of the calibration curve, respectively.

## 3. RESULTS AND DISCUSSION

### *3.1 Fabrication of PMDTO/RGO modified electrode*

As shown in Fig. 1, MDTO exhibited a much lower oxidation potential (0.19 V) in 0.1 M $LiClO_4$ aqueous solution than that in organic solvents, such as acetonitrile and propylene carbonate, in good agreement with our previous results [18]. For the preparation of PMDTO/GO/GCE, MDTO/GO was first electrochemically polymerized on the polished GCE in a homogeneous aqueous solution containing MDTO (0.01 M) and GO (2.0 mg $mL^{-1}$). Note that MDTO in the GO aqueous solution (Fig. 1B) showed an improved oxidation potential (0.36 V, extracted from first CV scan marked with red line in Fig. 1B) compared to MDTO in $LiClO_4$ aqueous solution (Fig. 1A). This could be attributed to the poor conductivity and ionization of GO. It is also found that the redox peak currents were less than that of PMDTO prepared in $LiClO_4$ aqueous solution. Furthermore, with the increase of time, a steady increase in the peak current density of the anode and cathodic during CV experiments implied an increasing amount of polymer film on the electrode surface. The redox peak of the polymer were broad, probably resulting from the broad distribution of polymer chain length and also the conversion of the conductive species on the polymer backbone from the neutral to metallic states [28,8].

In this case, GO was not only used as the supporting electrolyte, but also played an ingredient of the composite, which is attached to the PMDTO main chain during the CV scan. In the process of oxidative electropolymerization, GO could be merged with the polymer as the main counter ion,

because there were no additional dopants added to the dispersion of GO. Since the ionization of GO has electrostatic interaction with the radical generated by MDTO during electropolymerization, this effect facilitates the occurrence of polymerization and effectively reduced the potential required to form a polymer film [29,30]. To obtain the PMDTO/GO/GCE, PMDTO/GO was reduced by CV to get rid of instable oxygen-containing groups, which may reduce the selectivity for target molecules.

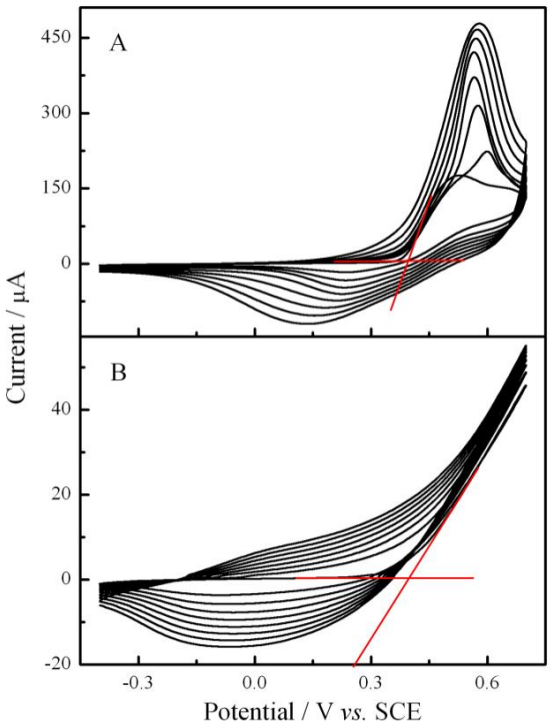


**Figure 1.** CVs of (A) 0.01 M MDTO in 0.1 M $LiClO_4$ aqueous solution and (B) 2.0 mg $mL^{-1}$ GO aqueous solution. Scan rate: 50 mV $s^{-1}$. Potential range: -0.4 ~ 0.7 V.

*3.2 Structure characterization*

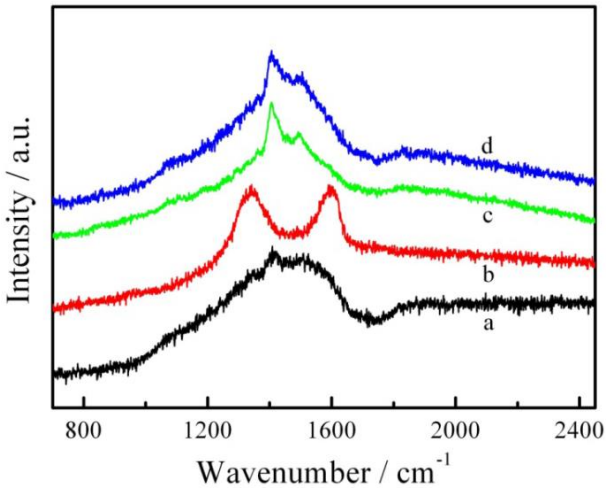


**Figure 2.** Raman spectra of PMDTO (a), GO (b), PMDTO/GO (c) and PMDTO/RGO (d).

Raman spectrum is applied to study the structures of the materials. In Fig. 2b, the D band and G band of GO can be observed at 1342 $cm^{-1}$ and 1590 $cm^{-1}$, corresponding to the defects of the GO and $sp^2$ carbon stretching modes, respectively. Compared to graphene oxide, PMDTO shows a broad absorption peak from 1414 to 1511 $cm^{-1}$ (Fig. 2a) [16,31]. As can be seen in Fig. 2c and Fig. 2d, PMDTO/GO and PMDTO/RGO exhibits similar absorption bands. Moreover, no obvious characteristic absorption of GO appeared in the spectra, suggesting that only tiny amounts of GO attached on PMDTO.

### *3.3 Surface morphology*

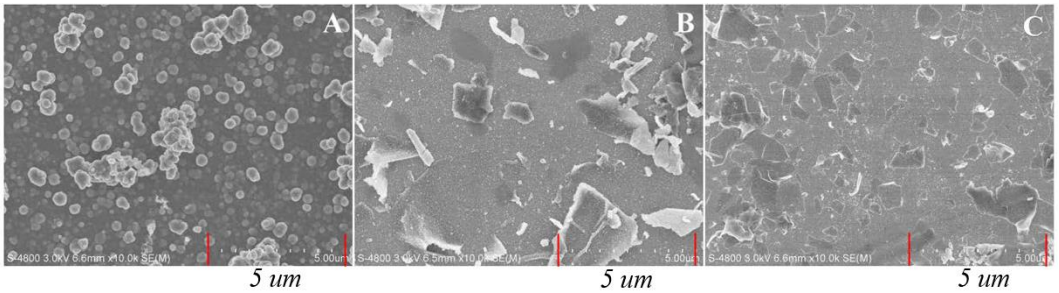


**Figure 3.** SEM images of PMDTO (A), PMDTO/GO (B) and PMDTO/RGO (C).

The surface morphology of PMDTO, PMDTO/GO and PMDTO/RGO was studied by SEM, respectively. As shown in Fig. 3A, the pure PMDTO showed disordered small granular-like polymer. The reason was probably that the monomers formed a layer of thin film firstly, and then formed polymer particles. In contrast, PMDTO/GO exhibited a more compact morphology substrate inserted/covered by plate-shaped GO sheets (Fig. 3B). After reduction, RGO plate-shaped sheets were distributed more evenly compared with PMDTO/GO film (Fig. 3C), which provided large specific area for the loading of IAA.

### *3.4 Electrochemical impedance spectroscopy (EIS)*

In order to investigate the interface properties of novel modified electrodes, EIS tests are performed in 5.0 mM $[Fe(CN)_6]^{3-/4-}$ containing 0.1 M KCl. As shown in Fig. 4, the $R_{et}$ of bare GCE was 450 Ω, while other modified electrodes showed very small electron transfer resistance (~0 Ω), indicating the improved conductivity due to the introduction of PMDTO. For the straight part at the low frequency, the phase angle of modified electrodes reached about $45^o$, which can be explained by favorable diffusion rate between the electrode and the solution. These features are helpful to improve the sensitivity of their-based electrochemical sensors.

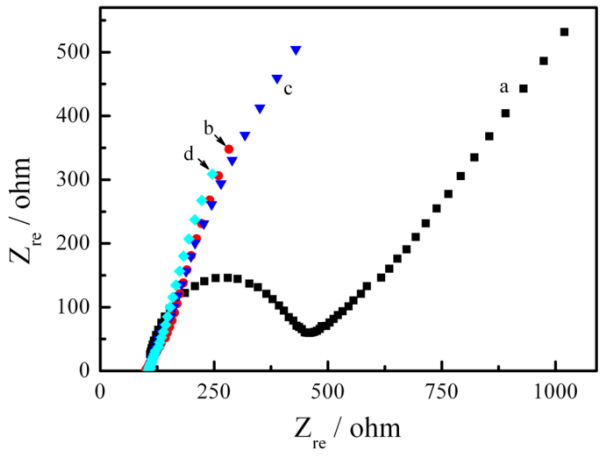


**Figure 4.** Nyquist plots of the bare GCE (a), PMDTO/GCE (b), PMDTO/GO/GCE (c) and PMDTO/RGO/GCE (d) in $[Fe(CN)_6]^{3-/4-}$ solution (5.0 mM) containing 0.1 M KCl. Frequency range: 0.1~$10^4$ Hz.

*3.5 Optimization of experimental conditions*

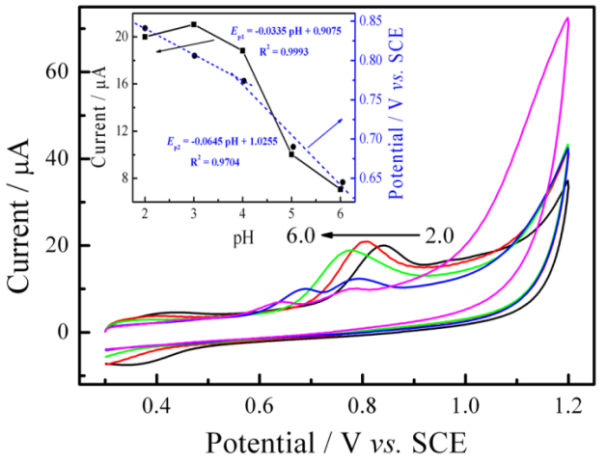


**Figure 5.** CVs at PMDTO/RGO/GCE in PBS with different pH values containing 0.05 mM IAA. Potentialscan rate: 100 mV $s^{-1}$. Inset: Effect of pH on anodic peak potentials and currents of IAA.

As shown in Fig. 5, with the increasing of pH, the oxidation peak current of IAA increased at first but then began to decrease at pH > 3.0. Especially, an abrupt current slump was observed in the range of 4.0~5.0 and the oxidation peak splited into two small peaks due to the ionization constant of IAA ($pK_a$ = 4.8). Moreover, the oxidation peak potential ($E_{pa}$) shifted negatively with increasing pH. Considering both response potential and peak current, subsequent analytical experiments were all performed in PBS (pH = 3.0).

*3.6 Electrochemical behavior*

Fig. 6 displays cyclic voltammograms (CVs) of GCE (a), PMDTO/GCE (b), MDTO/GO/GCE

(c) and PMDTO/RGO/GCE (d) in 0.05 mM IAA PBS (pH = 3.0). The peak current of the electrodes increased in the following order: GCE (a) < MDTO/GO (c) < PMDTO (b) < PMDTO/RGO (d). No obvious peak currents was found for bare GCE. This could be due to the sluggish electron transfer of bare GCE, suggested that the analyte is extremely difficult to undergo oxidative polymerization during the scanning process. In contrast, a larger oxidation peak current at 1.05 V can be observed on PMDTO/GCE, indicating that PMDTO possessed good catalytic effect for IAA, larger oxidation peak current corresponds to a two-electron and single proton oxidation reaction that produced a cation of 3-methyleneindolenine carboxylic acid. Similar phenomenon was reported and well explained in previous studies [32,33]. Compared with PMDTO modified electrode, PMDTO/GO/GCE exhibited a relatively lower response peak current, probably due to the low conductivity of GO. After the reduction of PMDTO/GO, however, the redox peak currents displayed a remarkable increase for the PMDTO/RGO. Furthermore, the response potential was shifted significantly to 0.78 V; the lower oxidation potential was favorable to improve the stability of PMDTO/RGO modified electrode.

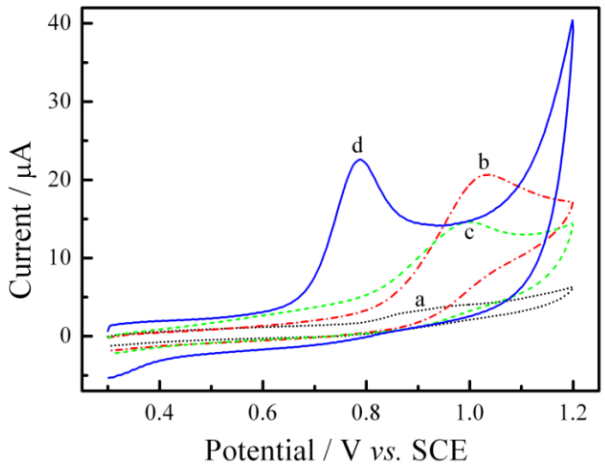


**Figure 6.** CVs of GCE (a), PMDTO/GCE (b), MDTO/GO/GCE (c) and PMDTO/RGO/GCE (d) in 0.05 mM IAA PBS (pH = 3.0). Potential scan rate: 100 mV $s^{-1}$.

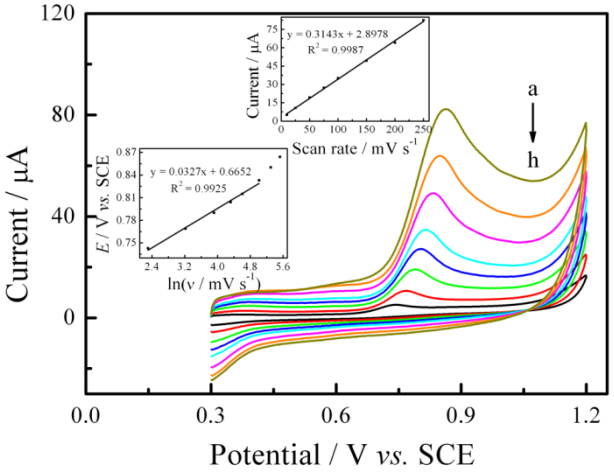


**Figure 7.** CVs of PMDTO/RGO/GCE in 0.05 mM IAA and 0.1 M PBS (pH = 3.0) at different scan rates: 250 (a), 200 (b), 150 (c), 100 (d), 75 (e), 50 (f), 25 (g), and 10 mV $s^{-1}$ (h).

In order to get insight into the reaction mechanism, the electrochemical behaviors of the PMDTO/RGO modified electrodes were studied by CV in 0.05 mM IAA aqueous solution. As shown in Fig. 7, the oxidation peak currents (*I*) were proportional to the scanning rate (*v*), and the linear equation can be expressed as: $I = 2.8978 + 0.3143\ v$ ($R^2 = 0.9987$) (inset of Fig. 7), indicating that the redox process of IAA on PMDTO/RGO modified GCE was non-diffusional and electroactive composites were adsorbed to the working electrode. Furthermore, a linear relationship between the natural logarithm of *v* and anodic peak potential was in the range of 25~250 mV $s^{-1}$ (Fig. 7), and the linear equation was $E_{pa} = 0.06652 + 0.0327 \ln v$ ($R^2 = 0.9925$). Based on Laviron's model, the electron transfer number (n) in the oxidation process of IAA was calculated to be around 2, in good agreement with previous results [8].

### *3.7 Determination of IAA*

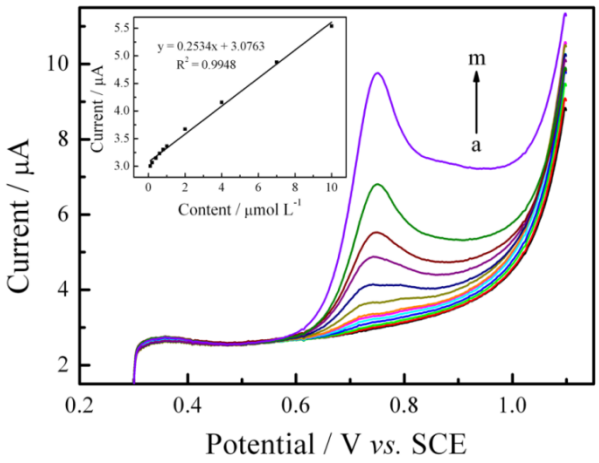


**Figure 8.** Linear sweep voltammetry of PMDTO/RGO/GCE in PBS (pH 3.0). The concentration of IAA: 0.1 (a), 0.2 (b), 0.4 (c), 0.6 (d), 0.8 (e), 1.0 (f), 2.0 (g), 4.0 (h), 6.0 (i), 8.0 (j), 10.0 (k), 20.0 (l), and 50.0 μM (m). Scan rate: 25 mV $s^{-1}$. Inset: plots of peak currents vs. concentration of IAA.

**Table 1.** Comparison of the fabricated sensors with previous reported results for the detection of IAA

| Fabricated sensors | Method | Liner range (μM) | LOD (μM) | Refs. |
|---|---|---|---|---|
| GCE | DPV | 1.8-660 | 2.7 | [26] |
| PEDOTM/GO/GCE | DPV<br>SWV | 0.6-10<br>0.05-40 | 0.087<br>0.033 | [8] |
| PMDTO/RGO/GCE | LSV | 0.1-10 | 0.03 | This work |

The calibration curves of IAA in PBS (pH = 3.0) were studied by linear sweep voltammetry under the optimized conditions. As shown in Fig. 8, the peak current (*I*) was positive in correlation

with the concentration of IAA (c) in the range of 0.1~10 μM. The linear relationship was expressed as: $I$ = 3.0763 + 0.2534 $c$ ($R^2$ = 0.9948), and the low detection limit (LOD) was estimated to be 0.03 μM (S/N = 3). Besides, a comparison between the obtained results and previous reports for the detection of IAA is summarized in Table 1. It also can be concluded that the detection of IAA on PMDTO/RGO/GCE can obtain a lower detection limit. Furthermore, the low detection potential can effectively avoid the interference from other species.

*3.8 Reproducibility and interference study*

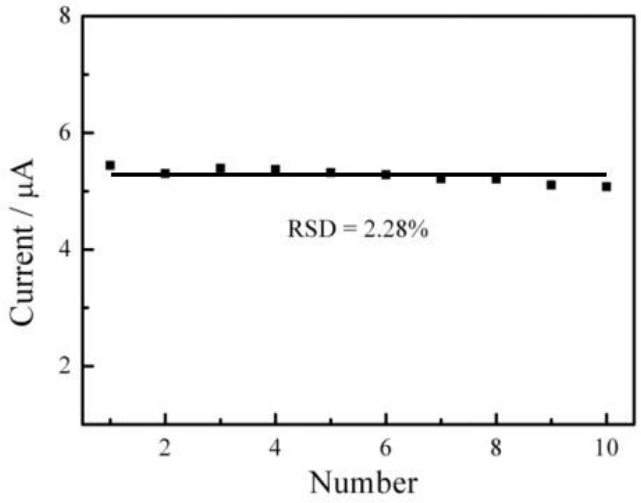


**Figure 9.** Reproducibility of PMDTO/RGO/GCE .

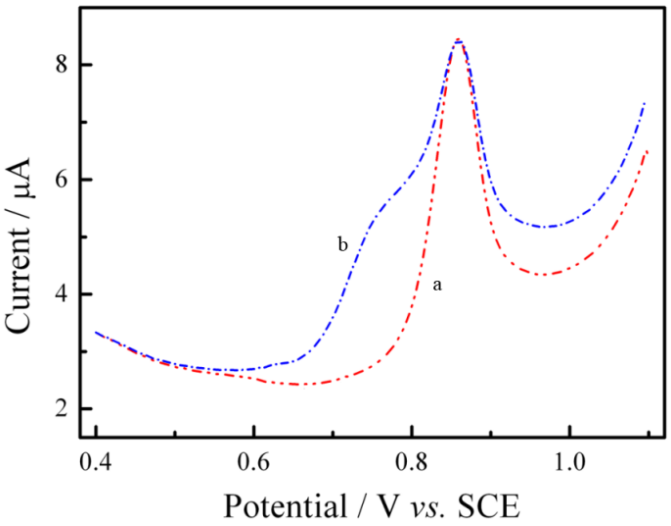


**Figure 10.** Interference of tyrosine (a) and tryptophan (b) for the detection of IAA at PMDTO/RGO/GCE in PBS (pH = 3.0). Potential scan rate: 100 mV $s^{-1}$.

The reproducibility of the fabricated sensor was carried out using 10 parallel modified electrodes in PBS (pH = 3.0) containing 10 μM IAA (Fig. 9). Clearly, there was no obvious change, and the relative standard deviation (RSD) was 2.28%, indicating that the fabricated sensor possessed

acceptable reproducibility.

Possible interferences were also studied by introducing them in PBS (pH = 3.0). The concentration of IAA and interfering ions were both fixed as 10 μM. The interferences including anions, hormones, cations, organic acids, carbohydrates, amino acids and vitamins, were investigated. It was found that the responses of the PMDTO/RGO modified electrode for 10 μM IAA were not influenced by all these additions except for tyrosine and tryptophan (Fig. 10). To improve the selectivity of the PMDTO/RGO modified electrode, further work can be focused on the design of new PMDTO derivatives with recognizable groups to specific compounds.

## 4. CONCLUSIONS

A composite based on PMDTO and RGO was facilely prepared through a two-step process: 1) low-potential electrochemical polymerization of MDTO in the homogeneous aqueous solution of MDTO and GO; 2) the electrochemical reduction of GO. As prepared PMDTO/RGO composite, combining with the advantages of RGO and PMDTO, exhibited large surface area, good conductivity and catalytic ability, and was successfully employed to fabricate an electrochemical sensor towards the detection of IAA. The fabricated sensor showed a lower response potential and obvious response signal to IAA. The high sensitivity, good stability and reproducibility of the sensor indicated that PMDTO could be utilized as a promising platform for electrochemical sensor.

ACKNOWLEDGEMENTS
This work is supported by the National Natural Science Foundation of China (51763010, 51863009), Science Foundation for Excellent Youth Talents in Jiangxi Province (20162BCB23053), the Key Research and Development Program of Jiangxi Province (20171BBH80007), the Natural Science Foundation of Jiangxi Province (20171BAB216018). J. X. thanks the financial support from the Innovation Driven “5511” Project of Jiangxi Province (20165BCB18016), and the Key Project of Natural Science Foundation in Jiangxi Province (20181ACB20010). X. L. thanks the Science and Technology Foundation of Jiangxi Educational Committee (GJJ160790). K. Q. thanks Jiangxi Educational Committee for a Postgraduate Innovation Program grant (YC2017-S409). N. J. thanks Jiangxi Science & Technology Normal University for a Postgraduate Innovation Program grant (YC2017X26).

## References

1. A. Santner, L. I. A. Calderon-Villalobos and M. Estelle, *Nat. Chem. Biol*, 5 (2009) 301.
2. C. Uggla, E. J. Mellerowicz and B. Sundberg, *Plant Physiol*, 117 (1998) 113.
3. S. Hou, J. Zhu, M. Ding and G. Lv, *Talanta*, 76 (2008) 798.
4. Y. Wu, B. Hu, *J. Chromatogr. A*, 1216 (2009) 7657.
5. Y. Zhou, Z. Xu, M. Wang, X. Meng and H. Yin, *Electrochim. Acta*, 96 (2013) 66.
6. Y. Yardım, M. E. Erez, *Electroanalysis*, 23 (2011) 667.
7. H. Yin, Z. Xu, Y. Zhou, M. Wang and S. Ai, *Analyst*, 138 (2013) 1851.
8. Z. L. Feng, Y. Y. Yao, J. K. Xu, L. Zhang, Z. F. Wang and Y. P. Wen, *Chin. Chem. Lett.*, 25 (2014) 511.
9. T. Gan, C. Hu, Z. Chen and S. Hu, *Talanta*, 85 (2011) 310.
10. Y. J. Yang, X. Xiong, K. Hou and S. Hu, *Russ. J. Electrochem.*, 47 (2011) 47.

11. K. Zhang, X. Duan, X. Zhu, D. Hu, J. Xu, L. Lu, H. Sun and L. Dong, *Synth. Met.*, 195 (2014) 36.
12. L. Zhang, Y. Wen, Y. Yao, J. Xu, X. Duan and G. Zhang, *Electrochim. Acta*, 116 (2014) 343.
13. W. Zhang, W. Zhang, Z. Xue, Y. Xue, N. Jian, K. Qu, S. Chen and J. Xu, *Electrochim. Acta*, 278 (2018) 313.
14. L. Zhang, Y. Wen, Y. Yao, X. Duan, J. Xu and X. Wang, *J. Appl. Polym. Sci.*, 130 (2013) 2660.
15. L. Dong, B. Lu, X. Duan, J. Xu, D. Hu, K. Zhang, X. Zhu, H. Sun, S. Ming, Z. Wang and S. J. Zhen, *Polym. Sci., Part A: Polym. Chem.*, 53 (2015) 2238.
16. E. Ermiş, D. Yiğit and M. Güllü, *Electrochim. Acta*, 90 (2013) 623.
17. Z. Feng, D. Mo, Z. Wang, S. Zhen, J. Xu, B. Lu, S. Ming, K. Lin and J. Xiong, *Electrochim. Acta*, 160 (2015) 160.
18. S. Ming, Z. Feng, D. Mo, Z. Wang, K. Lin, B. Lu and J. Xu, *Phys. Chem. Chem. Phys.*, 18 (2016) 5129.
19. A. I. Gopalan, N. Muthuchamy, S. Komathi and K. Lee. *Biosens. Bioelectron.*, 84 (2016) 53.
20. M. Raj, R. N. Goyal, *Sens. Actuators, B*, 233 (2016) 445.
21. H. Dai, N. Wang, D. Wang, H. Ma and M. Lin, *Chem. Eng. J.*, 299 (2016) 150.
22. J. Muñoz, L. J. Brennan, F. Céspedes, Y. K. Gun'ko and M. Baeza, *Compos. Sci. Technol.*, 125 (2016) 71.
23. E. T. Vilela Jr, R. C. S Carvalho, S. Y. Neto, C. S. Luz R and F. S. J. Damos, *Electroanal. Chem.*, 752 (2015) 75.
24. S. Kumar, S. Kumar, S. Srivastava, B. K. Yadav, S. H. Lee, J. G. Sharma, D. C. Doval and B. D. Malhotra, *Biosens. Bioelectron.*, 73 (2015) 114.
25. N. Hui, S. Wang, H. Xie, S. Xu, S. Niu and X. Luo, *Sens. Actuators, B*, 221 (2015) 606.
26. L. Wang, Y. Zhang, Y. Du, D. Lu, Y. Zhang and C. J. Wang, *J. Solid State Electrochem.*, 16 (2012) 1323.
27. J. Bulíčková, R. Sokolová, S. Giannarelli and B. Muscatello, *Electroanalysis*, 25 (2013) 303.
28. B. Lu, S. Zhen, S. Zhang, J. Xu and G. Zhao, *Polym. Chem.*, 5 (2014) 4896.
29. A. Österholm, T. Lindfors, J. Kauppila, P. Damlin and C. Kvarnstrom, *Electrochim. Acta*, 83 (2012) 463.
30. W. Si, W. Lei, Y. Zhang, M. Xia, F.Wang and Q. Hao, *Electrochim. Acta*, 85 (2012) 295.
31. K. Krishnamoorthy, M. Veerapandian, R. Mohan, K Sang-Jae, *Appl. Phys. A*, 106 (2012) 501.
32. T. Hu, G. J. Dryhurst, *J Electroanal. Chem.*, 362 (1993) 237.
33. K. Wu, Y. Sun and S. Hu, *Sens. Actuators, B*, 96 (2003) 658.